

## Thermodynamics of the 3D Hubbard Model on Approaching the Néel Transition

Sebastian Fuchs,<sup>1</sup> Emanuel Gull,<sup>2</sup> Lode Pollet,<sup>3</sup> Evgeni Burovski,<sup>4,5</sup> Evgeny Kozik,<sup>3</sup>  
Thomas Pruschke,<sup>1</sup> and Matthias Troyer<sup>3</sup>

<sup>1</sup>*Institut für Theoretische Physik, Georg-August-Universität Göttingen, 37077 Göttingen, Germany*

<sup>2</sup>*Department of Physics, Columbia University, New York, New York 10027, USA*

<sup>3</sup>*Theoretische Physik, ETH Zurich, 8093 Zurich, Switzerland*

<sup>4</sup>*LPTMS, CNRS and Université Paris-Sud, UMR8626, Bâtiment 100, 91405 Orsay, France*

<sup>5</sup>*Department of Physics, Lancaster University, Lancaster, LA1 4YB, United Kingdom*

(Received 24 September 2010; published 18 January 2011)

We study the thermodynamic properties of the 3D Hubbard model for temperatures down to the Néel temperature by using cluster dynamical mean-field theory. In particular, we calculate the energy, entropy, density, double occupancy, and nearest-neighbor spin correlations as a function of chemical potential, temperature, and repulsion strength. To make contact with cold-gas experiments, we also compute properties of the system subject to an external trap in the local density approximation. We find that an entropy per particle  $S/N \approx 0.65(6)$  at  $U/t = 8$  is sufficient to achieve a Néel state in the center of the trap, substantially higher than the entropy required in a homogeneous system. Precursors to antiferromagnetism can clearly be observed in nearest-neighbor spin correlators.

DOI: 10.1103/PhysRevLett.106.030401

PACS numbers: 05.30.Fk, 03.75.Ss, 71.10.Fd

The Hubbard model remains one of the cornerstone models in condensed matter physics, capturing the essence of strongly correlated electron physics relevant to high-temperature superconductors [1] and correlation-driven insulators [2]. While qualitative features of the phase diagram are known from analytical approximations, controlled quantitative studies in the low-temperature regimes relevant for applications are not readily tractable with tools presently available. A recent program that aims to implement the Hubbard model in a cold gases experiment [3] has led to experimental signs of the Mott insulator [4,5]. Modeling by the dynamical mean-field theory (DMFT) [5,6] and high-temperature series expansions (HTSE) [7] resulted in temperature and entropy estimates [8]. A major experimental achievement will be the detection of the antiferromagnetic phase, for which the slow and ill-understood equilibration rates, the limited number of detection methods, and inherent cooling problems will have to be overcome.

Experimental progress has also sparked interest in simulations of the 3D Hubbard model, where new algorithms, such as the real-space DMFT [9,10] and diagrammatic Monte Carlo [11] methods, have been developed. As in the case of bosons, where synergy between experiment and simulation has led to quantitative understanding of experiments [12], accurate results for the thermodynamics of the 3D Hubbard model will be important for validation, calibration, and thermometry of fermionic experiments. A crucial role is played by the entropy, since these experiments form isolated systems where parameters are changed adiabatically, not isothermally.

In this Letter, we provide the full thermodynamical equation of state of the Hubbard model—in particular,

the entropy, energy, density, double occupancy, and spin correlations—for interactions  $U$  up to the bandwidth  $12t$  on approach to the Néel temperature  $T_N$  by performing controlled large-scale cluster dynamical mean-field calculations and extrapolations to the infinite system size limit, as well as determinantal diagrammatic Monte Carlo (DMC) simulations at half filling. We use this information to calculate the entropy per particle required for experiments on ultracold atomic gases in optical lattices to reach a Néel state in the trap center. We finally show that the nearest-neighbor spin-correlation function contains clear precursors for antiferromagnetism that may already be detectable in current generation experiments and that are useful for thermometry (more so than measurements of the double occupancy) close to  $T_N$ .

The Hubbard model is defined by its Hamiltonian

$$\hat{H} = -t \sum_{\langle i,j \rangle, \sigma} \hat{c}_{i\sigma}^\dagger \hat{c}_{j\sigma} + U \sum_i \hat{n}_{i\uparrow} \hat{n}_{i\downarrow} - \sum_{i,\sigma} \mu_i \hat{n}_{i\sigma}, \quad (1)$$

where  $\hat{c}_{i\sigma}^\dagger$  creates a fermion with spin component  $\sigma = \uparrow, \downarrow$  on site  $i$ ,  $\hat{n}_{i\sigma} = \hat{c}_{i\sigma}^\dagger \hat{c}_{i\sigma}$ ,  $\langle \dots \rangle$  denotes summation over neighboring lattice sites,  $t$  is the hopping amplitude,  $U$  is the on-site repulsion, and  $\mu_i = \mu - V(\vec{r}_i)$  with  $\mu$  the chemical potential and  $V(\vec{r}_i)$  the confining potential at the location of the  $i$ th lattice site. We set  $V(\vec{r}) = 0$  in all calculations and consider realistic traps later on.

Our numerical approach is a cluster generalization of the DMFT [13]. In the cluster DMFT the self-energy is approximated by  $N_c$  momentum-dependent basis functions  $\phi_K(k)$ :  $\Sigma(k, \omega) \approx \sum_{K=1}^{N_c} \phi_K(k) \Sigma_K(\omega)$ . The exact problem is recovered for  $N_c \rightarrow \infty$ . Within the dynamical cluster approximation (DCA) [14] used here,  $\phi_K(k)$  are piecewise

constant over momentum patches, and DMFT [15] corresponds to  $N_c = 1$  and  $\Sigma = \Sigma(\omega)$ .

Solving the DMFT and DCA equations requires the solution of a quantum impurity model. Continuous-time quantum impurity solvers [16–18], in particular, the continuous-time auxiliary field method [17] with submatrix updates [19] used here, have made it possible to solve such models efficiently and numerically exactly on large clusters, thereby providing a good starting point for an extrapolation of finite-size clusters to the infinite system [11,20] We have performed extensive DCA calculations on bipartite clusters with  $N_c = 18, 26, 36, 48, 56,$  and  $64$ . In order to achieve an optimal scaling behavior we exclusively use the clusters determined in Ref. [20] following the criteria proposed by Ref. [21]. As the DCA exhibits a  $1/L^2$  finite-size scaling in the linear cluster size  $L = N_c^{1/3}$  away from critical behavior [22], we extrapolate our cluster results linearly in  $N_c^{-2/3}$ . DCA error bars include extrapolation uncertainties; a sample extrapolation is given in Ref. [23]. Despite a sign problem away from half filling, temperatures  $T/t \geq 0.4$ , on the order of the Néel temperature, are reliably accessible for all but the largest interaction strength  $U = 12t$  where we have been restricted to  $T/t \geq 0.5$ .

The potential energy, double occupancy, and nearest-neighbor spin-spin correlation have been measured directly. The kinetic energy  $E_{\text{kin}} = \sum_{\mathbf{n}, \vec{k}} \epsilon(\vec{k}) G(\vec{k}, i\omega_n)$  has been calculated by summing  $\epsilon(\vec{k})$ , the bare dispersion of the simple cubic lattice, and the single-particle Green function  $G(\vec{k}, i\omega_n)$  over all momenta  $\vec{k}$  and Matsubara frequencies  $i\omega_n$ . The entropy  $S$  has subsequently been calculated by numeric integration:

$$S(T) = S(T_u) - \frac{E(T_u)}{T_u} + \frac{E(T)}{T} - \int_T^{T_u} dT' \frac{E(T')}{T'^2}, \quad (2)$$

up to a  $T_u/t \approx 10$ , where the entropy  $S(T_u)$  is accurately given by HTSE. Tables of the complete results containing finite cluster and extrapolated values at and away from half filling for the entropy, energy, density, double occupancy, and spin correlations are given in the supplementary material [23].

*Results at half filling.*—We start our analysis at half filling and focus on  $U/t = 8$ , where a comparison with results from lattice simulations [24,25] is possible. We see in Fig. 1 that the entropy calculated by using the DCA and DMC simulations coincides within error bars at all temperatures. Agreement with a 10th order high-temperature series expansion [7] is found down to  $T/t \approx 1.6$ . At that temperature also the single-site DMFT starts to deviate because that method misses short-range antiferromagnetic correlations. The Néel temperature was found to be  $T_N/t \approx 0.36(2)$  in Ref. [20]. Our DMC calculations find it at  $T_N/t = 0.333(7)$ . By using the DCA, the critical entropy is  $s \approx 0.46(4)$  for  $T_N$  according to Ref. [20], and  $s := S/N_c \approx 0.42(2)$  with  $T_N$  according to the DMC simulations. We will use DMC numbers for  $T_N$  in the rest of this Letter.

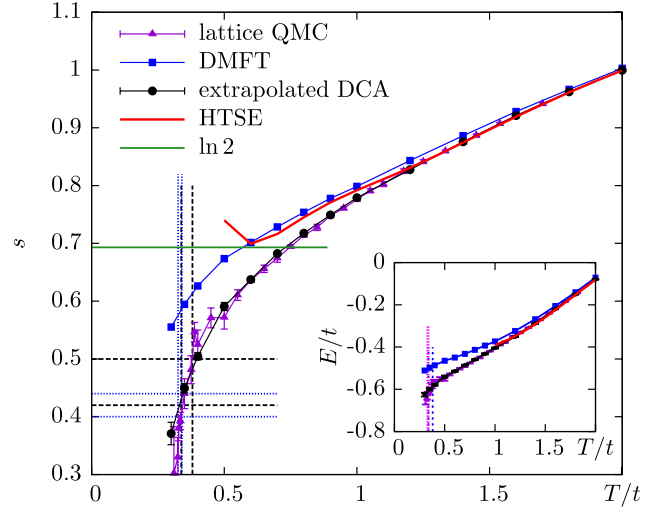


FIG. 1 (color online). Entropy per lattice site  $s$  of the Hubbard model as a function of temperature  $T/t$ , for  $U/t = 8$ , at half filling. Dashed vertical lines (black):  $T_N$  from Ref. [20]; dotted lines (blue): according to DMC simulations. Dashed horizontal lines (black): entropy per lattice site  $s$  at  $T_N$  [20]; dotted lines (blue): according to DMC simulations;  $\log(2)$  is shown as a solid (green) horizontal line. Inset: Energy  $E/t$  per lattice site. The DMC data were extrapolated linearly in  $1/L$  from the data at  $L = 6, 8, 10$ .

The *double occupancy*, which has played a crucial role in optical lattice experiments [4,5,7,26], is shown in Fig. 2 as a function of temperature at half filling for different values of  $U/t$ . While for small  $U/t$  a remarkable increase is seen on approach to  $T_N$ , only a plateau remains at moderate values of  $U/t$ . This is in contrast to the DMFT predictions but similar to lattice quantum Monte Carlo results in two dimensions [27]. For larger interactions ( $U/t \geq 12$ ), the double occupancy rises above that of a single-site paramagnet, consistent with DMFT results for

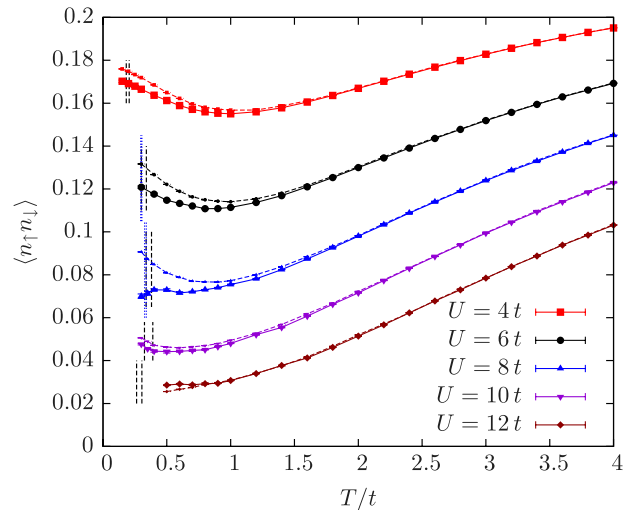


FIG. 2 (color online). Double occupancy of the Hubbard model as a function of  $T/t$ , at half filling. Extrapolated DCA results are shown as solid lines and DMFT values as dashed lines. Vertical lines: See Fig. 1.

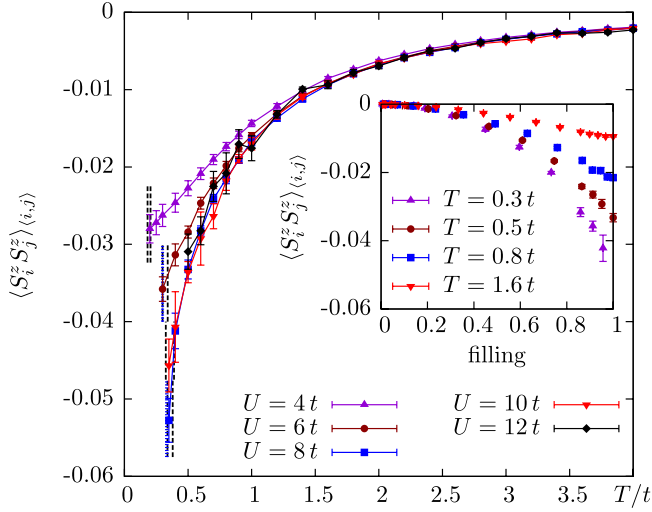


FIG. 3 (color online). Nearest-neighbor spin-spin correlation of the Hubbard model as a function of  $T/t$ , at half filling. Inset: Density dependence for  $U/t = 8$  and selected temperatures. Vertical lines: See Fig. 1.

the antiferromagnetic phase below  $T_N$  [10]. The negative slope of  $D(T)$ , discussed in the context of the single-site DMFT [28], persists for a wide range of parameters. Sharp features just above  $T_N$ , as detected in single-site (momentum-independent) studies [10], are not observed for the interaction values and temperature ranges studied here. Hence the proposal that the double occupancy is a good candidate for thermometry is not substantiated by more accurate momentum-dependent calculations.

The *spin-spin-correlation* function, plotted in Fig. 3 as a function of temperature for various  $U$  and as a function of filling for  $T/t = 0.3, 0.8$ , and  $1.6$  at  $U/t = 8$ , is accessible only in methods that include nonlocal correlations but may be accessible experimentally [29]. It has a steep slope on approach to the Néel temperature, which makes it an ideal quantity for thermometry.

*Results away from half filling.*—Figure 4 shows the entropy per lattice site for  $U/t = 8$ . The inset demonstrates

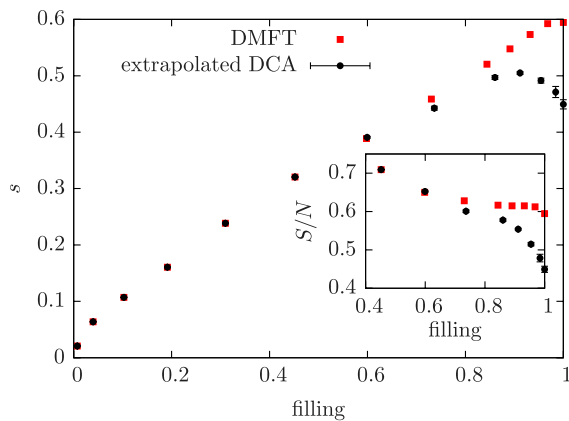


FIG. 4 (color online). Entropy per lattice site  $s$  and the entropy per particle  $S/N$  (inset) of the Hubbard model at the temperature  $T = 0.35t \approx T_N$ , as a function of density  $n$ , for  $U/t = 8$ .

that the entropy per particle number  $N$  increases strongly at lower densities. While the single-site DMFT remains accurate for densities  $n \lesssim 0.6$  due to the weak momentum dependence of the self-energy in this regime [30], the DCA results are important closer to half filling. Similarly, near half filling the DMFT overestimates the double occupancy by 10%, while deviations are less pronounced at lower densities. This observation persists for all interactions and temperatures investigated. The flattening of the double occupancy for  $8 \leq U/t \leq 12$  (cf. Fig. 2) is also seen away from half filling and leads to virtually unchanged profiles over the trap in an optical lattice system. On the other hand, the spin-spin-correlation function away from half filling (inset in Fig. 3) changes most rapidly near half filling when approaching  $T_N$  since it couples strongly to the developing (short-range) spin correlations.

*Entropy in the optical lattice system.*—We now turn to the experimentally relevant case of an optical lattice in a harmonic trap, which is a closed system where entropy is conserved. We choose parameters close to current experiments:  $V(\vec{r}) = 0.004(|\vec{r}|/a)^2 t$  with lattice spacing  $a$ , and we consider the case of half filling in the trap center:  $\mu = U/2$ . We treat the harmonic confinement in a local density approximation (LDA): For every site we perform a DCA simulation for a homogeneous system and average the results over the trap. LDA was found to be a good approximation for the Bose-Hubbard model for wide traps, except in close proximity to the critical point [31–33] of the  $U(1)$  phase transition because of the diverging correlation length. In our setup LDA errors are small compared to errors from the uncertainty of  $T_N$ .

Because of the large volume fraction, the wings of the gas may capture more entropy than the center of the trap, even though the entropy per site is comparable to the one in the center (see Fig. 5). In fact, the entropy of the whole density range  $0.1 < n < 0.9$  is large, and this opens the possibility to observe antiferromagnetic order in the trap center at an average entropy per particle over the

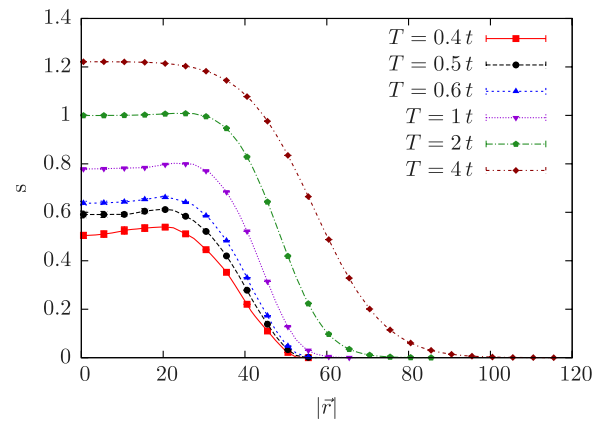


FIG. 5 (color online). Entropy profiles (entropy per lattice site) plotted over the trap in the LDA approximation for different temperatures with an interaction strength  $U/t = 8$ . Error bars, shown every 5 lattice spacings, are smaller than symbol size.

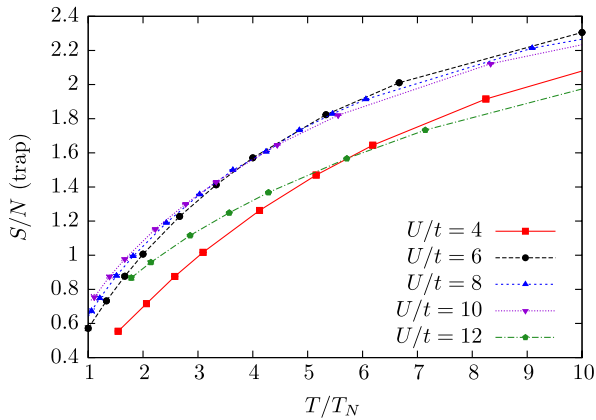


FIG. 6 (color online). Entropy per particle averaged over the trap as a function of temperature relative to  $T_N$  for different  $U$ . The Néel temperature is reached at  $T/t = 0.333(7)$  for  $U/t = 8$ , when the average entropy is  $S/N = 0.65(6)$ . Errors (not shown) in  $S(T_N)$  are estimated to be in the 10% range, with the largest contribution caused by the uncertainty in  $T_N$ .

trap which is about 50% larger than what could be expected from a homogeneous study. Optimal parameters are around  $U/t = 8$  when  $T_N/t = 0.333(7)$  according to DMC simulations, corresponding to  $S/N = 0.65(6)$  in the trap, while  $S/N = 0.42(2)$  would be expected for a homogeneous system. As seen in Fig. 6, all  $U$  in the range  $8 < U/t < 12$  lead to similar conclusions. We have verified that changing the trap by a factor of 4 does not alter these conclusions.

*Conclusions.*—We have provided the full thermodynamics of the 3D Hubbard model in the thermodynamic limit by using the DCA formalism for  $U/t \leq 12$  and temperatures above the Néel temperature. Comparing to single-site DMFT results we found that the latter already fail at remarkably high temperatures ( $T/t \approx 1.5$  for  $U/t = 8$  at the 1% level) near half filling. While the entropy per particle at the Néel temperature  $T_N/t = 0.333(7)$  (determined with DMC simulations) is  $S/N = 0.42(2)$  for  $U/t = 8$  in a homogeneously half filled system, we find that the Néel transition in a trap can already be reached at  $S/N = 0.65(6)$  in a realistically sized harmonic trap (taking  $T_N$  according to Ref. [20] leads to  $S/N = 0.69$ ).

We have also investigated the double occupancy and the nearest-neighbor spin-spin-correlation function as experimentally measurable quantities that were suggested to show precursors of antiferromagnetism. The double occupancy is almost flat as a function of temperature, while the spin correlations show a strong temperature dependence around the Néel temperature. This suggests that the spin correlations, not the double occupancy, are best suited to observe precursors of antiferromagnetism and measure the temperature. Our numerical data can be used to calibrate such a spin-correlation thermometer.

We acknowledge stimulating discussions with I. Bloch, T. Esslinger, A. Georges, D. Greif, O. Parcollet, V. Scarola,

and L. Tarruell. This work was supported by the Swiss National Science foundation, the National Science Foundation Grants No. DMR-0705847 and No. PHY-0653183, ANR Grant No. ANR-BLAN-6238, the Aspen Center for Physics, a grant from the Army Research Office with funding from the DARPA OLE program, and by the DFG through the collaborative research center SFB 602. We used the Brutus cluster at ETH Zurich and Norddeutscher Verbund für Hoch- und Höchstleistungsrechnen. Simulation codes were based on Algorithms and Libraries for Physics Simulations [34]. While finalizing this Letter, we became aware of a related effort [35] using the DMFT and HTSE.

- [1] P. W. Anderson, *Science* **235**, 1196 (1987).
- [2] M. Imada, A. Fujimori, and Y. Tokura, *Rev. Mod. Phys.* **70**, 1039 (1998).
- [3] M. Köhl *et al.*, *Phys. Rev. Lett.* **94**, 080403 (2005).
- [4] R. Jördens *et al.*, *Nature (London)* **455**, 204 (2008).
- [5] U. Schneider *et al.*, *Science* **322**, 1520 (2008).
- [6] L. De Leo *et al.*, *Phys. Rev. Lett.* **101**, 210403 (2008).
- [7] V. W. Scarola *et al.*, *Phys. Rev. Lett.* **102**, 135302 (2009).
- [8] R. Jördens *et al.*, *Phys. Rev. Lett.* **104**, 180401 (2010).
- [9] M. Potthoff and W. Nolting, *Phys. Rev. B* **59**, 2549 (1999).
- [10] E. V. Gorelik *et al.*, *Phys. Rev. Lett.* **105**, 065301 (2010).
- [11] E. Kozik *et al.*, *Europhys. Lett.* **90**, 10004 (2010).
- [12] S. Trotzky *et al.*, *Nature Phys.* **6**, 998 (2010).
- [13] T. Maier *et al.*, *Rev. Mod. Phys.* **77**, 1027 (2005).
- [14] M. H. Hettler *et al.*, *Phys. Rev. B* **58**, R7475 (1998).
- [15] A. Georges *et al.*, *Rev. Mod. Phys.* **68**, 13 (1996).
- [16] A. N. Rubtsov, V. V. Savkin, and A. I. Lichtenstein, *Phys. Rev. B* **72**, 035122 (2005).
- [17] E. Gull *et al.*, *Europhys. Lett.* **82**, 57003 (2008).
- [18] P. Werner *et al.*, *Phys. Rev. Lett.* **97**, 076405 (2006).
- [19] E. Gull *et al.*, arXiv:1010.3690.
- [20] P. Kent *et al.*, *Phys. Rev. B* **72**, 060411(R) (2005).
- [21] D. D. Betts and G. E. Stewart, *Can. J. Phys.* **75**, 47 (1997).
- [22] T. A. Maier and M. Jarrell, *Phys. Rev. B* **65**, 041104 (2002).
- [23] See supplemental material at <http://link.aps.org/supplemental/10.1103/PhysRevLett.106.030401> for all raw data of the 3D Hubbard model computed with various methods for several interaction strengths.
- [24] R. Staudt, M. Dzierzawa, and A. Muramatsu, *Eur. Phys. J. B* **17**, 411 (2000).
- [25] E. Burovski *et al.*, *Phys. Rev. Lett.* **101**, 090402 (2008).
- [26] N. Strohmaier *et al.*, *Phys. Rev. Lett.* **104**, 080401 (2010).
- [27] T. Paiva *et al.*, *Phys. Rev. Lett.* **104**, 066406 (2010).
- [28] F. Werner *et al.*, *Phys. Rev. Lett.* **95**, 056401 (2005).
- [29] S. Trotzky *et al.*, *Phys. Rev. Lett.* **105**, 265303 (2010).
- [30] E. Gull *et al.*, *Phys. Rev. B* **82**, 155101 (2010).
- [31] S. Wessel *et al.*, *Phys. Rev. A* **70**, 053615 (2004).
- [32] M. Campostrini and E. Vicari, *Phys. Rev. Lett.* **102**, 240601 (2009); *Phys. Rev. A* **81**, 023606 (2010).
- [33] L. Pollet, N. V. Prokof'ev, and B. V. Svistunov, *Phys. Rev. Lett.* **104**, 245705 (2010).
- [34] A. F. Albuquerque *et al.*, *J. Magn. Magn. Mater.* **310**, 1187 (2007).
- [35] L. De Leo *et al.*, arXiv:1009.2761 [Phys. Rev. A (to be published)].